



Co-published by
Institute of Fluid-Flow Machinery
Polish Academy of Sciences
Committee on Thermodynamics and Combustion
Polish Academy of Sciences

Copyright©2024 by the Authors under license CC BY 4.0

<http://www.imp.gda.pl/archives-of-thermodynamics/>



Research on optimization of the heating system in buildings in cold regions by energy-saving control

Wanting He^a, Hai Huang^{b*}

^aChongqing Industry Polytechnic College, Yubei, Chongqing 401120, China

^bChongqing Vocational Institute of Engineering JiangJin Chongqing 402260, China

*Corresponding author email: huanglia826@yeah.net

Received: 06.09.2023; revised: 17.10.2023; accepted: 10.01.2024

Abstract

Building heating is an indispensable part of people's winter life in cold regions, but energy conservation and emission reduction should also be taken into account during the heating process. This paper provides a concise overview of the heating system based on air-source heat pump radiant floor and its control strategy. It also optimizes a control system based on thermal comfort and energy efficiency ratio, and analyzes a room in Xining City, Qinghai Province, to test the heating system performance under two control strategies. The final results show that under the traditional control strategy, the cumulative working time of the heating system within a day was 15 hours, the average indoor temperature was 17.36°C, the temperature standard deviation was 2.08°C, and the average power consumption was 189.6 kWh. Under the improved control strategy, the cumulative working time of the heating system within a day was reduced to 10 hours, the average indoor temperature was 18.56°C, the temperature standard deviation was 0.92°C, and the average power consumption was 132.5 kWh.

Keywords: Building heating; Cold region; Energy efficiency control; Radiant floor

Vol. 45(2024), No. 1, 129–135; doi: 10.24425/ather.2024.150445

Cite this manuscript as: He, W.T., & Huang, H. (2024). Research on optimization of the heating system in buildings in cold regions by energy-saving control. *Archives of Thermodynamics*, 45(1), 129–135.

1. Introduction

With the swift progress of the economy and the enhancement of individuals' quality of life, building heating has become an indispensable part of life in cold regions during winter [1]. However, the traditional heating method mainly relies on fossil fuels such as coal and fuel oil, which has a significant negative impact on the environment [2]. The substantial carbon dioxide emissions not only exacerbate global warming but also directly threaten human health. Therefore, optimizing the heating systems in buildings located in cold regions to reduce energy consumption and environmental pollution has become one of the urgent challenges in today's society [3]. Moreover, with the in-

creasing awareness of energy saving and environmental protection, precise control of heating systems and maximizing energy utilization can be achieved through the introduction of intelligent control systems and the utilization of renewable energy sources. Katić et al. [4] introduced a machine learning approach to develop predictive models for managing an individualized heating system. The experiments revealed that the participants experienced consistent comfort levels during the trial, and they expressed contentment with the automated regulation. Gupta et al. [5] proposed a heating controller based on deep reinforcement learning, aiming to enhance occupants' thermal comfort and minimize energy costs in smart buildings. Additionally, Kaminska [6] examined the influence of occupant behaviour on

He W.T., Huang H.

Nomenclature

c_p	– specific heat capacity of the water circulated by the pump between the condenser and the radiant floor, J/(kg K)
C	– convective heat transfer between the individual and their surroundings, W/m ²
COP	– coefficient of performance
f_{cl}	– clothing coefficient of the human body
f_{eff}	– correction coefficient of the body movement
G	– volumetric flow rate of the circulating water, m ³ /s
h_c	– convective heat transfer coefficient, W/(m ² K)
M	– heat power emitted at the surface by the body due to metabolism, kW
P	– power of the input energy, kW
P_a	– partial pressure of steam in the air associated with the relative humidity, Pa
Q_h	– output heat of the air source heat pump, kW

R	– radiant heat transfer between individual and their surroundings, W/m ²
t_a	– average temperature of the air, °C
t_{cl}	– temperature on the surface of the garment, °C
t_{in}	– temperature of the incoming water from the radiant floor flowing back to the condenser, °C
t_{out}	– temperature of the outgoing water from the condenser flowing to the radiant floor, °C
PMV	– average thermal comfort
T_{cl}	– absolute temperature at the body surface, K
\bar{T}_r	– average absolute temperature in the environment, K
W	– heat power emitted at the surface by the body due to work, kW

Greek symbols

ε	– human body surface heat transfer rate
ρ	– density of the circulating water, kg/m ³
σ	– Stefan-Boltzmann constant, W/(m ² K ⁴)

energy usage in existing public buildings in Poland and conducted an experimental evaluation. They found that occupants perceived a broad range of temperature settings as thermally comfortable and a 1°C reduction in the temperature set point could result in energy savings of about 5%. This paper briefly introduced a heating system based on an air-source heat pump radiant floor and its control strategy. It adopted thermal comfort and energy efficiency ratio as the basis for optimizing the control. Furthermore, a case study of a room in Xining City, Qinghai Province, was carried out to test the heating performance of the heating system under two control strategies.

2. Heating system optimization based on energy-saving control

2.1. Heating system based on air-source heat pump floor radiation

A building heating system is a facility and equipment used to provide heat to a building during the cold season. It mainly comprises components such as heating equipment, heat transfer medium, heating pipe network, and a control system [7]. The heating equipment serves as the core component responsible for supplying heat, while the heat transfer medium facilitates the effective transfer of heat energy from the heating equipment to all areas of the building through circulating flow. The heating pipe network forms the network system for transmitting and distributing the heat medium within the building heating system. Finally, the control system assumes a crucial role within the building heating system [8], as it allows for precise regulation of indoor temperature by controlling the heating equipment, heat transfer medium, and heating pipe network. This control system plays a pivotal role in realizing the overall heating system's control strategy.

The heating equipment heat source can be categorized into three types: solar heat source, air heat source and geothermal heat source. Among them, the solar heat source is relatively more energy-saving and environmentally friendly; however, its dependency on sunlight makes it less stable for heating. Alt-

hough a geothermal heat source is both energy-efficient and environmentally friendly, it requires the installation of heat pumps deep underground, which poses significant construction challenges. On the other hand, the air heat source absorbs heat from the surrounding air [9], providing both stability and ease of installation. In addition to the heat source, there are different kinds of heating ends in the building heating system, including fan coils, radiators and radiant floors. Fan coils achieve heat transfer by forcing indoor air convection through blowing, while radiators transfer heat through natural convection. Radiant floors achieve heat transfer through heat radiation [10]. Compared to the first two heating ends, radiant floor heating is not only quieter but also offers a more uniform heat distribution. Figure 1 presents a schematic diagram of an air-source heat pump radiant floor heating system.

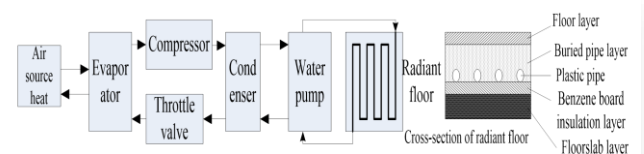


Fig. 1. Schematic diagram of the heating system with air-source heat pump floor radiation.

In this particular system, the evaporator utilizes a liquid medium for heat transfer, which effectively captures thermal energy from the air heat source and undergoes a phase change into a gaseous state [11]. The gaseous medium is then compressed in the compressor, further raising its temperature. Subsequently, the compressed medium condenses back into a liquid form in the condenser. The heat in the medium is transferred to the condensing water in the condenser, and the liquid medium cycles back into the evaporator through a throttle valve to absorb heat again. The process repeats. The condensed water, which absorbs heat in the condenser, is pumped into pipes buried in the radiant floor. The heat within the condensing water is then radiated indoors through the floor and subsequently returned to the condenser for further heat absorption [12].

The structure of the radiant floor is presented in Fig. 1, showing a hierarchical composition comprising multiple layers positioned in a top-to-bottom sequence. The first layer is the floor layer, which serves as a decorative structural layer and can be made of materials such as wood or tiles, possessing heat transfer properties. Moreover, the materials have a certain level of heat resistance [13] and do not release harmful substances to the human body when subjected to heat. The second layer is the buried pipe layer, primarily consisting of concrete made from crushed stone. This layer serves as the bed for laying the plastic pipes used for heat transfer. Typically, these plastic pipes are positioned at the lowermost part of the buried pipe layer to optimize the upward conduction of heat. Next, there is the benzene board insulation layer, which provides excellent heat insulation properties, preventing the downward transfer of heat. The final layer is the floor slab layer, acting as the supporting surface of the room.

2.2. Optimization of control strategies for heating systems

To optimize the energy-saving effect of the heating system during operation, in addition to adjusting the structural composition of the heating system [14], energy conservation and emission reduction can also be achieved through the optimization of the system control strategy. The traditional control strategy for an air-source heat pump radiant floor heating system is relatively straightforward in principle. It treats the evaporator, compressor, condenser, throttle valve [15] and water pump as components of a unified air-source heat pump. The control strategy involves maintaining the heat pump workload by monitoring the difference between the return water temperature of the heat pump and the desired temperature. Specifically, when the return water temperature surpasses the maximum set value, measures are taken to decrease the heat pump workload such as reducing the operation of the water pump or compressor and closing off the throttle valve. On the other hand, when the temperature of the returning water drops below the predetermined minimum threshold [16], the heat pump's workload is increased by elevating the workload of the water pump or compressor and opening the throttle valve.

The traditional control strategy, though relatively simple in

principle and implementation, may not be suitable for effectively controlling the radiant floor heating system owing to the thermal inertia exhibited by both the floor and the building envelope. The real-time change in indoor temperature cannot be accurately reflected by the variation in return water temperature. Consequently, there may be situations where the indoor temperature is already adequate, yet heat transfer persists due to a lack of corresponding adjustment in the return water temperature. This situation can lead to both heat wastage and discomfort for occupants as indoor temperatures continue to rise [17]. When controlling and regulating the heating system, it is essential to take into account not just the energy-saving effectiveness but also the comfort of the inhabitants. Therefore, in this paper, the control strategy is optimized from two perspectives: the energy

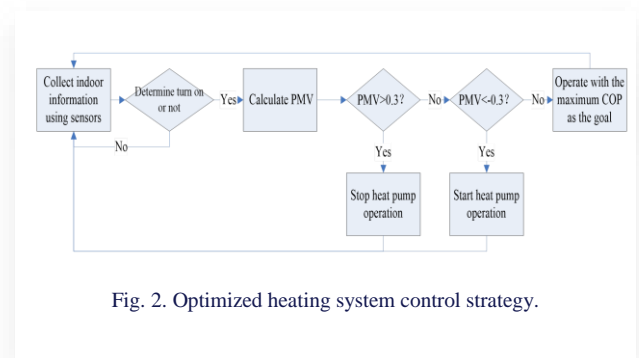


Fig. 2. Optimized heating system control strategy.

efficiency of the heating system and thermal comfort. The optimized control strategy is depicted in Fig. 2.

According to this:

1. Various sensors installed in the room are utilized to collect information about the room, including room temperature, relative humidity and the number of people in the room.
2. When no one is indoors, the heat provided by the air conditioner is equivalent to waste [18], so first determine whether the heating system is on according to whether there is someone indoors (if there is someone indoors, turn on the system and go to the next step; if there is no one indoors, turn off the system and go back to step 1).
3. The indoor environmental data collected by the sensors are utilized to calculate the indoor thermal comfort [19]. The corresponding formula is:

$$PMV = (0.303e^{-0.036M} + 0.028)((M - W) - 3.05 \times 10^{-3}(5733 - 6.99(M - W) - P_a) - 0.42((M - W) - 58.15) - 1.7 \times 10^{-5}M(5867 - P_a) - 0.0014M(34 - t_a) - R - C) \quad (1a)$$

$$R = \varepsilon f_{cl} f_{eff} \sigma (T_{cl}^4 - \bar{T}_r^4), \quad (1b)$$

$$C = f_{cl} h_c (t_{cl} - t_a), \quad (1c)$$

where: PMV represents the average thermal comfort, M represents the heat power emitted at the surface by the body due to metabolism, W represents the heat power emitted at the surface by the body due to work, P_a represents the partial pressure of steam in the air, which is associated with the relative humidity, t_a is the average temperature of the air, R represents the quantity of radiant heat transfer between individ-

ual and their surroundings, C represents the quantity of convective heat transfer between the individual and their surroundings, ε is the human body surface heat transfer rate, f_{cl} denotes the clothing coefficient of the human body, f_{eff} is the correction coefficient of the body movement, σ represents the Stefan-Boltzmann constant, T_{cl} is the absolute temperature on the body surface, \bar{T}_r is the average absolute temper

He W.T., Huang H.

ature in the environment, h_c represents the convective heat transfer coefficient [20], and t_{cl} represents the temperature at the surface of the garment.

4. Whether the indoor thermal comfort is greater than 0.3 is judged. If it is greater than 0.3, it means that the indoor temperature is too hot for the body to feel uncomfortable, then stop the heat pump and return to step 1; otherwise, go to the next step.
5. Whether the indoor thermal comfort is less than -0.3 is judged. If it is less than -0.3 , it means that the indoor temperature is low and makes people feel uncomfortable, then turn on the heat pump and go back to step 1; on the contrary, go to the next step.
6. When the thermal comfort is between -0.3 and 0.3 , the indoor temperature is in line with the human comfort feeling. At this time, it is necessary to make the heating system operate with the minimum waste of energy. This paper adopts *COP* to measure the energy efficiency ratio of the heating system, which is the ratio of the output heat to the input energy. The larger the value, the less the energy is wasted. The specific formula is:

$$COP = Q_h/P \quad (2a)$$

$$Q_h = \frac{c_p \rho G (t_{out} - t_{in})}{3600} \quad (2b)$$

where: P is the power of the input energy, Q_h is the output heat of the air source heat pump, c_p is the specific heat capacity of the water being circulated by the pump between the condenser and the radiant floor, ρ is the density of the circulating water, G is the volumetric flow rate of the circulating water, t_{out} stands for the temperature of the outgoing water from the condenser flowing to the radiant floor, and t_{in} is the temperature of the incoming water from the radiant floor flowing back to the condenser. The heating system operates at the maximum *COP* as its goal. Finally, it returns to step 1.

3. Example analysis

3.1. Objects of analysis

The room tested is located in Xining City, which is the capital city of Qinghai Province. The climate of Xining City is influenced by the Tibetan Plateau and the Asian monsoon, showing a typical plateau climate. The local summer is relatively short and mild, while the winter is long, from November to March. Winter temperatures are low, usually around 0°C during the day and dropping below -10°C at night, often accompanied by snowfall. Due to the influence of the Tibetan Plateau, Xining City has a large daily difference in temperature and a significant difference between daytime and nighttime temperatures, and can be considered a cold region.

The basic structure of the room used for the test is illustrated in Fig. 3, which is divided into a large and a small area. The large area is 6.0×3.5 m, and the small area is 2.0×1.5 m. The wall-to-window ratio is 0.3. Walls have a heat transfer coefficient of $0.45 \text{ W}/(\text{m}^2 \text{ K})$. The roof has a heat transfer coefficient of $0.25 \text{ W}/(\text{m}^2 \text{ K})$.

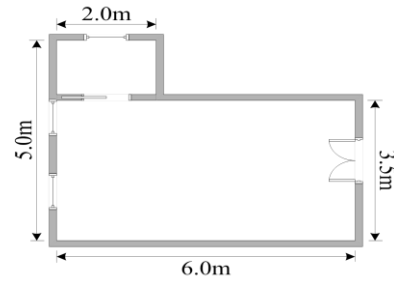


Fig. 3. Basic structure of the test room.

3.2. Equipment parameters

Air-source heat pump related parameters: the rated input power of the compressor was equal to 2.5 kW, with a displacement of 46.5 cm^3 and a refrigerant dosage of 2 kg. The evaporator was of the finned type, and its copper tube had an outer diameter of 9.52 mm, a thickness of 0.5 mm, and a length of 5 m. The rated input power for the fan was 90 W. The expansion valve was an externally balanced valve. The condenser was a pipe heat exchanger, and its outer seamless tube had a diameter of 35 mm and a thickness of 1.5 mm. The inner tube was made of smooth copper and has an outer diameter of 31 mm, a thickness of 0.8 mm, and a length of 4.2 m.

Water pump-related parameters: the water tank was of the pressure-resistant type with a capacity of 0.2 m^3 ; the water pump was centrifugal with a rated power of 320 W, a maximum flow rate of $9 \text{ m}^3/\text{h}$, and a head of 5 m.

Radiant floor: the floor slab layer is 120 mm thick and has a thermal conductivity of $1.75 \text{ W}/(\text{m K})$; the benzene board insulation layer is 13 mm thick and has a thermal conductivity of $0.05 \text{ W}/(\text{m K})$; the buried pipe layer is 28 mm thick and has a thermal conductivity of $0.94 \text{ W}/(\text{m K})$; the floor layer is 18 mm thick and has a thermal conductivity of $0.94 \text{ W}/(\text{m K})$; the buried pipe layer contains heat-conducting water pipes composed of crosslinked polyethylene material, with a water pipe diameter measuring 20 mm.

3.3. Test methods

Firstly, temperature and humidity sensors were installed on the walls around the room at intervals of 0.6 m both vertically and horizontally, totalling 45 sensors, and their data were intercommunicated with the data of the heat pump host. The traditional control strategy was also tested in this test to further validate the enhanced control strategy optimization capabilities.

The traditional control strategy is as follows. The outlet water temperature t_{out} of the air-source heat pump was set to 50°C . The inlet water temperature t_{in} was set to 45°C . When t_{in} was higher than 45°C , the heat pump host was turned off gradually, and when t_{in} was lower than 45°C , the heat pump host was turned on gradually.

The improved strategy was as described above. The air-source heat pump was regulated according to the indoor *PMV* as well as the heating system *COP*. The heat pump outlet temperature t_{out} was also set to 50°C .

In conducting the test, the heating system under each control strategy was operated alternately for a time limit of one day (implement a control strategy for a consecutive day, followed by a pause in operation for the next day; then, adopt an alternative control strategy for another consecutive day and again pause operations on a subsequent day). Temperature sensors set up inside and outside of the room were used to collect the average temperature changes indoors and outdoors. The settings of indoor environmental parameters are presented in Table 1. The energy consumption of the heating system during one day was recorded. The experiment was conducted for a total of 12 days, and the results for each day were averaged.

Table 1. Indoor environmental parameters during testing.

Parameters, hours	8:00–20:00	20:00–8:00
Indoor temperature, °C	20	18
Relative humidity, %	30	30
Number of people indoors (n)	10	2

3.4. Test results

The test recorded the heat pump working status of the heating system every one hour. In the recorded data, a value of "1" indicated that the heat pump was running, while a value of "0" signified that the heat pump was stopped. Figure 4 illustrates the changes in the heat pump operating state in one day under the two control strategies. Table 2 shows the accumulated working time of the heating system within one day under the two control strategies.

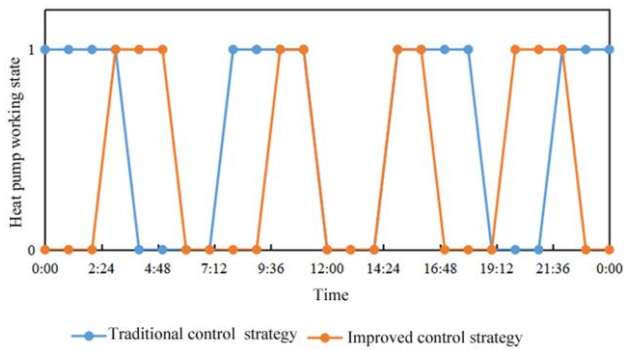


Fig. 4. Heat pump operating state of the heating system in a day under two control strategies.

Table 2. The accumulated working time of the heating system within one day under the two control strategies.

Parameter	Traditional control strategy	Improved control strategy
Accumulated working time within one day, h	15	10

It can be seen from Table 2 and Fig. 4 that both control strategies resulted in intermittent heating, indicating energy-saving characteristics for both approaches. However, the improved control strategy led to a reduced cumulative running time for the heat pump compared to the traditional control strategy.

Figure 5 displays the changes in indoor temperature as well as outdoor temperature in one day under both control strategies. Table 3 presents the statistics of indoor temperature changes under the two control strategies. It is evident from Table 3 and Fig. 5 that, regardless of the control strategies employed, the heating system effectively sustained an indoor temperature considerably above that of the outdoor environment. However, when comparing the indoor temperature under the two strategies, it was observed that while the traditional control strategy resulted in significant fluctuations in indoor temperature, the improved strategy maintained a relatively stable temperature around 18°C, with only slight fluctuations.

Table 3. Statistics of indoor temperatures under the two control strategies.

Parameter	Traditional control strategy	Improved control strategy
Average indoor temperature, °C	17.36	18.56
Highest indoor temperature, °C	21.03	20.01
Indoor lowest temperature, °C	13.01	17.02
Standard deviation of indoor temperature, °C	2.08	0.92

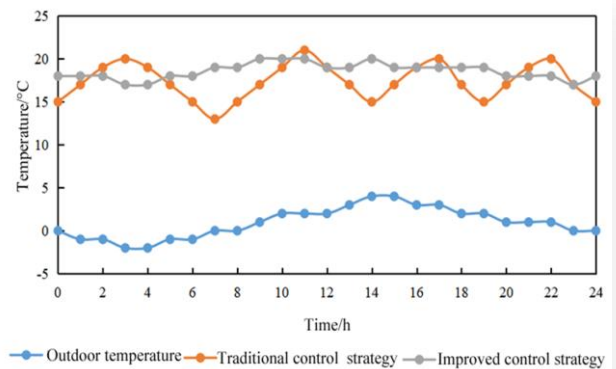


Fig. 5. Variation of indoor temperature as well as outdoor temperature in a day under two control strategies.

The average power consumption of the system in a day under the two control strategies is shown in Fig. 6. The heating system consumed an average of 189.6 kWh per day with the traditional strategy, whereas the improved strategy resulted in an average power consumption of 132.5 kWh for the heating system. It was intuitively seen from Fig. 6 that the heating system under the improved control strategy consumed less power.

The reasons for the above results were analyzed. The traditional strategy gradually adjusted the heat pump host based on variations in the temperature of the returning water. Although there might be shutdown conditions resulting in less than 24 hours of operation time, the heat pump host was regulated step by step while the heat pump continued to run during this process. In contrast, the improved control strategy determined when to switch on/off the heat pump host based on the comfort level, and even within the range of human comfort, it operated with the maximum *COP* as a goal.

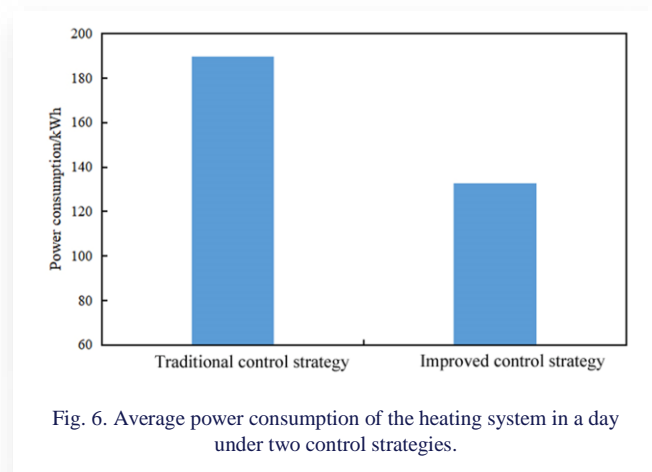


Fig. 6. Average power consumption of the heating system in a day under two control strategies.

Using the comfort level as a regulatory basis considered the thermal inertia of the envelope, which reduced the operating time and naturally resulted in less power consumption.

4. Conclusion

This paper briefly introduced the heating system that utilizes air-source heat pump radiant floor technology and its control strategy and used thermal comfort as well as energy efficiency ratio as the basis to optimize the control. Then, a case study was carried out with a room in Xining City, Qinghai Province, to evaluate the heating efficiency of the heating system under the two control strategies. The results obtained are as follows:

1. The heat pump of the system had intermittent heating under both control strategies, and the cumulative running time of the heat pump under the improved control strategy was less than that under the traditional strategy.
2. The indoor temperature was maintained at a level higher than the outdoor temperature by both control strategies employed for the heating system, but the heating system under the improved strategy provided a more stable indoor temperature.
3. The average power consumption of the heating system in a day was 189.6 kWh under the traditional strategy and 132.5 kWh under the improved strategy.

In conclusion, when using an air-source heat pump radiant floor heating system in cold regions, intermittent heating can be employed with the duration adjusted based on thermal comfort guidelines to achieve energy savings and emission reductions. The future research direction of this study is to further optimize the control strategy of the heating system for better regulation.

References

- [1] Wathan, N. (2021). Multi-zone heating control benefits. *Heating Ventilating & Plumbing*, 42(2), 42.
- [2] Polyakov, S., Akimov, V., & Polukazakov, A. (2020). Simulation of the heating control system of a smart apartment building. *Modeling of Systems and Processes*, 13(1), 68–76. doi: 10.12737/2219-0767-2020-13-1-68-76
- [3] Kim, S.H., Chung, K.S., & Kim, Y.I. (2015). Thermal Comfort Range of Radiant Floor Heating System by Residential Style. *Transactions of the Korea Society of Geothermal Energy Engineers*, 11(1), 7–14. doi: 10.17664/ksgee.2015.11.1.007
- [4] Katić, K., Li, R., Verhaart, J., & Zeiler, W. (2018). Neural network based predictive control of personalized heating systems. *Energy & Buildings*, 174, 199–213. doi: 10.1016/j.enbuild.2018.06.033
- [5] Gupta, A., Badr, Y., Negahban, A., & Qiu, R.G. (2020). Energy-Efficient Heating Control for Smart Buildings with Deep Reinforcement Learning. *Journal of Building Engineering*, 34(C), 101739. doi: 10.1016/j.job.2020.101739
- [6] Kaminska, A. (2019). Impact of Heating Control Strategy and Occupant Behavior on the Energy Consumption in a Building with Natural Ventilation in Poland. *Energies*, 12(22), 1–18. doi: 10.3390/en12224304
- [7] Du, Y. (2014). Feasibility Analysis of Radiant Floor Cooling and Heating System Applications. *Applied Mechanics and Materials*, 716–717, 428–430. doi: 10.4028/www.scientific.net/AMM.716-717.428
- [8] Ma, H., Li, C., Lu, W., Zhang, Z., Yu, S., & Du, N. (2016). Experimental study of a multi-energy complementary heating system based on a solar-groundwater heat pump unit. *Applied Thermal Engineering*, 109, 718–726. doi: 10.1016/j.applthermaleng.2016.08.136
- [9] Yu, B.H., Seo, B.M., Moon, J.W., & Lee, K.H. (2015). Analysis of the Part Load Ratio Characteristics and Gas Energy Consumption of a Hot Water Boiler in a Residential Building under Korean Climatic Conditions. *Korean Journal of Air Conditioning & Refrigeration Engineering*, 27(9), 455–462. doi: 10.6110/KJACR.2015.27.9.455
- [10] Woodson, R. (2015). Radiant Floor Heating, Second Edition. *JAMA: the Journal of the American Medical Association*, 313(1), 93–94.
- [11] Yang, E. (2015). Research on Control Property of Low-Temperature Floor Radiant Heating System. *Open Construction & Building Technology Journal*, 9(1), 311–315.
- [12] Hong, S.K., & Cho, S.H. (2015). The Experimental Study of the Heat Flux and Energy Consumption on Variable Flow Rate for Secondary Side of DHS. *Korean Journal of Air-Conditioning and Refrigeration Engineering*, 27(5), 247–253. doi: 10.6110/KJACR.2015.27.5.247
- [13] Shaw, B.H. (2018). Infection in Mental Hospitals, with Special Reference to Floor Treatment. *Journal of Mental Science*, 69, 24–45. doi: 10.1192/bjp.69.284.24
- [14] Kim, S.H., Chung, K.S., & Kim, Y.I. (2015). Thermal Comfort Range of Radiant Floor Heating System by Residential Style. *Transactions of the Korea Society of Geothermal Energy Engineers*, 11(1), 7–14.
- [15] Toyoda, S., Fujiwara, T., Uchida, A., & Ishibashi, J. (2016). ESR dating of sea-floor hydrothermal barite: contribution of ²²⁸Ra to the accumulated dose. *Nephron Clinical Practice*, 43(1), 201–206. doi: 10.1515/geochr-2015-0042

- [16] Kong, Q.X., Feng, J., & Yang, C.L. (2017). Numerical Simulation of a Radiant Floor Cooling Office Based on CFD-BES Coupling and FEM. *Energy Procedia*, 105, 3577–3583.
- [17] Barzin, R., Chen, J.J.J., Young, B.R., & Farid, M.M. (2015). Application of PCM underfloor heating in combination with PCM wallboards for space heating using price based control system. *Applied Energy*, 148(1–2), 39–48. doi: 10.1016/j.apenergy.2015.03.027
- [18] Bae, W.B., Ko, J.H., Mun, S.H., & Huh, J.H. (2015). An Occupants' Location-Driven Control of Radiant Floor Heating Using Fingerprinting Method in Residential Buildings. *Journal of the Architectural Institute of Korea Planning & Design*, 31(11), 211–219.
- [19] Bellos, E., & Tzivanidis, C. (2017). Energetic and financial sustainability of solar assisted heat pump heating systems in Europe. *Sustainable Cities and Society*, 33, 70–84. doi: 10.1016/j.scs.2017.05.020
- [20] Singh, S.B., Vummadisetti, S., & Chawla, H. (2017). Influence of Curing on the Mechanical Performance of FRP Laminates. *Journal of Building Engineering*, 16, 1–19. doi: 10.1016/j.job.2017.12.002